ISSN 1674-1056
http://cpb.iphy.ac.cn
http://iopscience.iop.org/cpb
中国物理 B
Chinese Physics
中国物理 Chinese Physics B

Josephson effect in the strontium titanate/lanthanum aluminate junction

Xing Yang(阳星), Jie Chen(陈杰), Yabin Yu(余亚斌), Quanhui Liu(刘全慧)
Citation: Chin. Phys. B . 2019, 28(9): 097401 . **doi:** 10.1088/1674-1056/28/9/097401
Journal homepage: http://cpb.iphy.ac.cn; http://iopscience.iop.org/cpb

What follows is a list of articles you may be interested in

Topological phase diagrams and Majorana zero modes of the Kitaev ladder and tube

Yiming Wang(王一鸣), Zhidan Li(李志聃), Qiang Han(韩强)
Chin. Phys. B . 2018, 27(4): 047401 . **doi:** 10.1088/1674-1056/27/4/047401

Comparison of band structure and superconductivity in $FeSe_{0.5}Te_{0.5}$ and FeS

Yang Yang(杨阳), Shi-Quan Feng(冯世全), Yuan-Yuan Xiang(向圆圆), Hong-Yan Lu(路洪艳), Wan-Sheng Wang(王万胜)
Chin. Phys. B . 2017, 26(12): 127401 . **doi:** 10.1088/1674-1056/26/12/127401

Topological phase transition in a ladder of the dimerized Kitaev superconductor chains

Bo-Zhen Zhou(周博臻), Bin Zhou(周斌)
Chin. Phys. B . 2016, 25(10): 107401 . **doi:** 10.1088/1674-1056/25/10/107401

Novel 0-π transitions in Josephson junctions between noncentrosymmetric superconductors

Jun-Feng Liu(刘军丰), Huan Zhang(张欢), Jun Wang(汪军)
Chin. Phys. B . 2016, 25(9): 097403 . **doi:** 10.1088/1674-1056/25/9/097403

Field-dependent resistive transitions in $Yba_2Cu_3O_{7-\delta}$ thin films: Influence of the pseudogap on vortex dynamics

S H Naqib, R S Islam
Chin. Phys. B . 2015, 24(1): 017402 . **doi:** 10.1088/1674-1056/24/1/017402

Josephson effect in the strontium titanate/lanthanum aluminate junction*

Xing Yang(阳星)†, Jie Chen(陈杰), Yabin Yu(余亚斌), and Quanhui Liu(刘全慧)

School of Physics and Electronics, Hunan University, Changsha 410082, *China*

(Received 28 February 2019; revised manuscript received 26 June 2019; published online 7 August 2019)

We report theoretical studies on the newly discovered novel Josephson effect and scanning tunneling spectroscopy (STS) at the interface of strontium titanate/lanthanum aluminate (STO/LAO). With a phenomenological boson–fermion model, the density of states is calculated and the results are consistent with the STS experiments. A typical calculation of Josephson effect is performed, and it is in qualitative agreement with the experiments. The calculations indicate that the gap states come from the pairing of quasi-particles with a finite total momentum and the Josephson current comes from the tunneling of quasi-particle pairs with zero momentum. The quasi-particles are Bogoliubov quasi-particles. Moreover, the fits using Kulik's formula imply that the Josephson junction at the STO/LAO interface has a point contact with the clean superconductor limit.

Keywords: strontium titanate/lanthanum aluminate, Josephson effect, scanning tunneling spectroscopy, pseudogap

PACS: 74.20.–z, 74.25.F–, 74.50.+r **DOI:** 10.1088/1674-1056/ab33f4

1. Introduction

The superconductivity of strontium titanate (STO) was discovered in the 60s[1] and the interests to understand the microscopic origin last over five decades. Its distinctions to other types of superconductors include its large insulating band gap,[2] pseudo-gap behavior[3] at low temperature, etc. One of its special properties is that, as the most dilute superconductor, its Fermi energy $E_{\rm F} \sim 1$ meV[4] is small compared to its Debye energy $\omega_{\rm D} \sim 5$ meV.[5] The characteristics forbid the applications of the BCS theory, which demands the retardation condition $\omega_{\rm D} \ll E_{\rm F}$.

In order to explain the origin of electron pairing, some theoretical explanations have been proposed. Arce-Gamboa applied the ϕ^4 theory of phonons and proposed the pairing origin to be the interactions with local phonons.[6] Edge related the soft-mode optical phonons to electron doping and the density functional theory calculations showed that the ferroelectric fluctuations were the pairing glue in the doped STO.[7] Kedem suggested a ferroelectric mode mediated electron pairing.[8] While, Ruhman described a plasmon-mediated superconductivity.[9] For the pseudogap behavior, Liu explained it by the local states near impurities.[10] In the experiments, the magnitude of superconducting gap Δ can be measured by the spectral tunneling spectroscopy (STS)[3] and its phase by the Josephson effects.[11] Experiments of angle-resolved photon emission spectroscopy (ARPES) are very helpful for testing the theories, however, the demands for low temperature (< 1 K) set restrict conditions for the ARPES experiments. On the other hand, with the ARPES experiment, one can answer interesting questions as what is the dispersion of the quasi-particles, and the spectral function can be extracted and used as evidences for theories.

Furthermore, the electron pairs without superconductivity are found in the STO system.[12,13] This leads us to construct a phenomenological boson–fermion model, in which the superconducting quasiparticles, hard-core bosons, and the interaction between them are included. Here, the bosons are the electron pairs not necessarily with superconductivity, which are robust above the superconducting transition temperature.[12,13] Due to its small size, it is modeled as a bosonic field $b_{\boldsymbol{k}}$. Based on our model, the calculated density of states is in quantitative agreement with the experimental data.[3] Moreover, the theoretical calculations show that the critical current in the Josephson effect is proportional to the superconducting gap, and the gap contains $\langle \hat{b}_0^\dagger \rangle$, where $\hat{b}_0^\dagger$ is the annihilation operator of the quasi-particle pair with zero momentum. This indicates that the depletion of Cooper pairs can decrease the superconducting gap and Josephson current. Furthermore, the fit by Kulik's formula implies that the two-dimensional electron system at the STO/LAO interface is a clean superconductor.

In Section 2, we present the boson fermion model to describe the Josephson tunneling. The methods and approximations to solve the model Hamiltonian are shown in Section 3. We analyze the results and show what can be known from the phenomenological model in Section 4. In Section 5, we draw our conclusion and raise the possible unsolved questions.

*Project supported by the National Natural Science Foundation of China (Grant No. 11675051) and China Scholarship Council (Grant No. 201506130054).

†Corresponding author. E-mail: yangxing@hnu.edu.cn

© 2019 Chinese Physical Society and IOP Publishing Ltd

2. Model

The Hamiltonian of a junction is supposed to have three terms

$$\hat{H} = \hat{H}_{\rm L} + \hat{H}_{\rm R} + \hat{H}_{\rm T}, \tag{1}$$

where $\hat{H}_{\rm L,R}$ is the Hamiltonian of the left or right lead. $\hat{H}_{\rm T}$ is the Hamiltonian that couples them

$$\hat{H}_{\rm T} = \sum_{\boldsymbol{k},\boldsymbol{q},\sigma} (T_{\boldsymbol{k}\boldsymbol{q}} \hat{c}^{\dagger}_{\boldsymbol{q}{\rm R}\sigma} \hat{c}_{\boldsymbol{k}{\rm L}\sigma} + {\rm H.c.}), \tag{2}$$

where $\hat{c}_{\boldsymbol{q}{\rm L,R}\sigma}$ is the annihilation operator of an electron with momentum $\boldsymbol{q}$ and spin σ in the left or right lead and $T_{\boldsymbol{k}\boldsymbol{q}}$ represents the strength of the tunneling from the left lead with a momentum $\boldsymbol{k}$ to the right lead with a momentum $\boldsymbol{q}$.

The lead's Hamiltonian, $\hat{H}_{\rm L}$ or $\hat{H}_{\rm R}$, is composed of two parts

$$\hat{H}_{\rm L,R} = \hat{H}_{0,{\rm L,R}} + \hat{H}_{1,{\rm L,R}}, \tag{3}$$

with

$$\hat{H}_0 = \sum_{\boldsymbol{k},\sigma} E_{\boldsymbol{k}} \hat{\gamma}^{\dagger}_{\boldsymbol{k},\sigma} \hat{\gamma}_{\boldsymbol{k},\sigma} + \sum_{\boldsymbol{q}} \xi_{\boldsymbol{q}} \hat{b}^{\dagger}_{\boldsymbol{q}} \hat{b}_{\boldsymbol{q}}, \tag{4}$$

$$\hat{H}_1 = \sum_{\boldsymbol{k},\boldsymbol{q}} \frac{V_1(\boldsymbol{k},\boldsymbol{q})}{\sqrt{S\rho}} \hat{b}^{\dagger}_{\boldsymbol{q}} \hat{\gamma}_{-\boldsymbol{k}+\frac{\boldsymbol{q}}{2}\downarrow} \hat{\gamma}_{\boldsymbol{k}+\frac{\boldsymbol{q}}{2}\uparrow} + {\rm H.c.}, \tag{5}$$

where $\hat{b}_{\boldsymbol{k}}$ ($\hat{b}^{\dagger}_{\boldsymbol{k}}$) is the annihilation (creation) operator of a hard-core boson and $\hat{\gamma}_{\boldsymbol{k}}$ ($\hat{\gamma}^{\dagger}_{\boldsymbol{k}}$) annihilates (creates) a superconducting quasiparticle. $E_{\boldsymbol{k}} = \sqrt{\varepsilon_k^2 + \Delta_0^2}$, $\varepsilon_{\boldsymbol{k}} = \hbar^2 k^2/2m^* - \mu$, m^* is the effective mass of the electron, μ is the electrochemical potential and is negligible. Here we want to point out that H_1 represents the interaction between the superconducting quasiparticles and the non-superconducting electron pair, which may come from the direct and indirect interactions between the electrons. The surface area $S \approx 10^5$ nm^2, the carrier density $\rho \approx 10^{13}$ cm^{-2}, and $\xi_q = \hbar v|q|$, where $v = 0.073c$ and c is the speed of light in vacuum. The bosonic field represents the electron pairs in both superconducting state and normal state. Δ_0 is the energy gap at 0 K and it includes both the superconducting gap and the energy gap $\Delta_{\rm p}$. Experiments show that $\Delta_{\rm p}$ remains finite when the temperature is higher than the superconducting transition temperature.[3] The quasi-particle annihilation operator $\gamma_{\boldsymbol{k}}$ is connected with the bare electron operator through Bogoliubov transformation.[14]

The interaction potential is

$$V_1 = V_{\rm c} \sqrt{\frac{1}{2\pi|q|L}} \sqrt{\frac{(\xi_{\boldsymbol{q}} - E_{\boldsymbol{q}-\boldsymbol{k}})^2}{(\xi_{\boldsymbol{q}} - E_{\boldsymbol{q}-\boldsymbol{k}})^2 + \Delta_0^2}}, \tag{6}$$

where $q_{\rm min} = \Delta_0/(\hbar v)$, and L is the characteristic length of the system and is approximately 30 nm in the case. The two-dimensional model can be connected with a one-dimensional case, with the relation $L = S/(2\pi L')$, where S is the surface area of the two-dimensional electron system (2DES) and L' is the length in the one-dimensional case. $V_{\rm c}$ is a phenomenological parameter, which is from $\mathcal{O}(0.1$ eV) to $\mathcal{O}(1$ eV) and $V_{\rm c} = 0$ corresponds to the typical BCS superconductors. The phenomenological parameter $V_{\rm c}$ directly results in the decay rate Γ and the gap states. V_1 is not allowed to be in the form of a constant or q^{α}, since both of them will close the zero-width gap, which contradicts with the experiments.[12,15]

When $q = 0$, V_1 is set to be a constant

$$V_1 = V_{\rm s}. \tag{7}$$

The parameters $V_{\rm c}$ and $V_{\rm s}$ can be determined by STS and Josephson tunneling, respectively. The $V_{\rm s}$ represents the coupling between the zero-momentum electron pairs and electrons, which is analogous to the phonon–electron coupling constant in the BCS theory. The form of the phenomenological interaction potential comes from the fit with the experiments.

3. Method

The parity of electrons and holes is not obvious, since STO can be n-doped or p-doped, while the model can be easily extended to the doped cases. Moreover, the perturbation theory is applied and we take the first order approximation (see Appendix A). Furthermore, the local self-energy approximation is used within the perturbation theory. This means $\Sigma(k) \approx \Sigma(k = 0)$. With the increase of k, $\Sigma(k)$ decreases monotonically, which means that the density of states is overestimated with the approximation.

The calculations of Josephson tunneling are mostly consistent with the typical Green's function technique[16] (see Appendix B).

4. Result

Figure 1[15] shows an unconventional superconducting feature. When $V_{\rm c}$ is small, the graph shows a singularity-like peak, which resembles the BCS case. As $V_{\rm c}$ increases, the more gap states appear and it transits to an unconventional superconducting phase. The result agrees well with the experiments[3] at $V_{\rm c} \sim 0.02$ a.u.

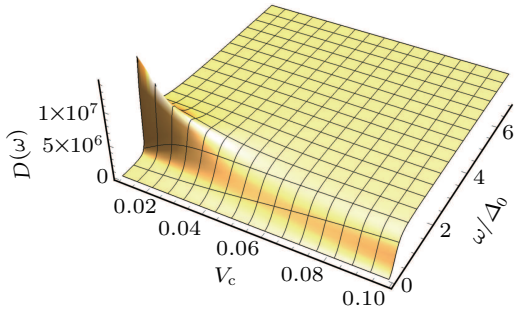


Fig. 1. The density of states, $D(\omega)$, is plotted along with the variation of $V_{\rm c}$; $D(\omega)$ and $V_{\rm c}$ are in atomic units.

The particles along the direction perpendicular to the surface are supposed to be confined in a parabolic potential $\frac{1}{2}m\omega^2 z^2$, and its quantum number is n_z, the density of states $D(E) = n_z(E)D_{2D}$, where $E = E_{\parallel} + E_z$ and $E_z = (1/2+n_z)\hbar\omega$. When E increases, $n_z(E)$ changes from n to $n+1$, and the electrons have a new plane in momentum space to occupy, $D(E)$ increases from nD_{2D} to $(n+1)D_{2D}$, in which $D_{2D} = m^*S/\pi\hbar^2$, where m^* is the effective mass and S is the area of the 2D surface.

For the fit with the boson–fermion model, the superconducting gap $\Delta_s \approx 0.2$ neV. The value is small compared to the experimental result, which is $\Delta_s \approx 40$ μeV. If the 2DES at the STO/LAO interface is assumed to be a clean superconductor and the Josephson junction has a point contact, the Kulik's formula Eq. (B18) can be applied and the superconducting gap is fitted as $\Delta_s \sim 1$ μeV.

Figure 2 shows a step-like conductance and critical current as n_z increases. The electrochemical potential μ is larger as E_z increases and $E_z = (1/2+n_z)\hbar\omega$, so a larger μ results in a greater n_z and n_z can be viewed as a measure of the gate voltage V_{sg}. Figure 2 is in quantitative agreement with the experiments.[11]

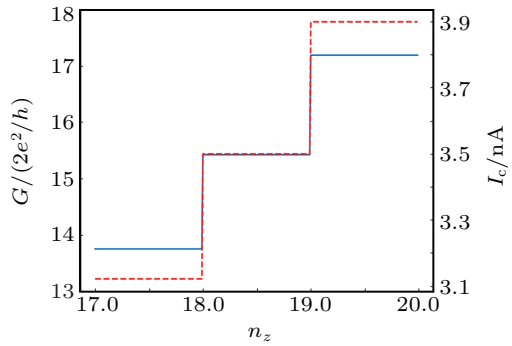


Fig. 2. The blue solid line represents the conductance in normal states and the red dashed line is the critical current. n_z is the number of modes in the perpendicular direction. Both the boson–fermion model and Kulik's formula can result in the I_c–n_z curve.

5. Conclusion

We proposed a two-component boson–fermion model with s-wave superconducting order parameter. Within the model, the feature of the density of states of the unconventional superconducting material STO/LAO can be explained. It suggests that the gap states come from the pairing of quasi-particles and the electrons in the superconducting phase are Bogoliubov quasi-particles. The calculated density of states is in quantitative agreement with the STS experiments. Besides, if the increase of the magnetic field can reduce the lifetime of quasi-particle pairs, then we argue that it can reduce the gap states, which can be tested in future experiments.

Furthermore, we calculated the Josephson effect at the STO/LAO interface. The calculated results for the Josephson effect in the STO/LAO interface are in quantitative agreement with the experimental curves of current–voltage and conductance–voltage. It shows that the Josephson critical current is proportional to the superconducting gap, which is due to the condensation of quasi-particles into pairs with zero momentum.

Moreover, the Kulik-formula fit of Josephson effect is also in agreement with the experimental I_c–V_g curve and superconducting order parameter, which suggests that the Josephson junction at the STO/LAO interface has a point contact in the clean superconductor limit.

The model is phenomenological, but it can predict the density of states fairly well and may provide a hint to the origin of electron pairing in STO.

Appendix A

With Matsubara formalism, we make the simplest first order approximation to the self-energy of the Bogoliubov quasi-particles and the self-energy is

$$\Sigma(\boldsymbol{k},\omega) = \int \frac{S|V_1(\boldsymbol{k},\boldsymbol{q})|^2 \mathrm{d}\boldsymbol{q}}{2\pi n_0\hbar^2} \frac{1}{\omega - (\xi_{\boldsymbol{q}} - E_{\boldsymbol{q}-\boldsymbol{k}})/\hbar + \mathrm{i}\eta} \times \left(\frac{1}{\exp\beta\xi_{\boldsymbol{q}} - 1} + \frac{1}{\exp\beta E_{\boldsymbol{q}-\boldsymbol{k}} + 1}\right), \quad \text{(A1)}$$

where S is the surface area of the conductive regions at the STO/LAO interface. Here, we apply a technique that evaluates V_1 from δ function first and later assumes the self-energy is k-independent and $\Sigma(\boldsymbol{k},\omega) = \Sigma(0,\omega)$, which means that the self-energy is local, since the Fourier transform of $\Sigma(0,\omega)$ is proportional to $\delta(x)$ in the real space, where $\delta(x)$ is a Dirac function. With the approximation, the decay rate is defined as

$$\Gamma(\omega) \equiv \mathrm{Im}\Sigma(0,\omega). \quad \text{(A2)}$$

With the Kramers–Krönig relation and the hole–particle symmetry,

$$\Sigma'(\omega) = \mathrm{Re}(\Sigma(0,\omega)) = \frac{2\omega}{\pi}\mathrm{P}\int_0^{\infty} \frac{\Gamma(\omega')}{\omega'^2 - \omega^2}\mathrm{d}\omega'. \quad \text{(A3)}$$

The numerical calculations show $\Sigma'(\omega) \ll \Delta_0$ at low temperature and is negligible.

The density of states is defined as

$$D(\omega) = \int \frac{S}{4\pi^2} A(\boldsymbol{k},\omega)\mathrm{d}\boldsymbol{k}, \quad \text{(A4)}$$

where $A(\boldsymbol{k},\omega) = \frac{1}{\pi}\mathrm{Im}(G(\boldsymbol{k},\omega))$ and $G = \frac{1}{\mathrm{i}\omega - E_{\boldsymbol{k}}/\hbar - \mathrm{i}\Gamma}$. We can get the analytic form of the density of states (see Appendix C). The density of states of holes can be inferred from that of the electrons by $D(\omega) = D(-\omega)$ with the assumption of particle–hole symmetry.

Appendix B

The Josephson current is calculated at $T = 0$ K and voltage $V_e = 0$ V and the calculation and notation follow those presented in Ref. [16]. The current is

$$I = e\langle \dot{\hat{N}}_R \rangle. \tag{B1}$$

where

$$\hat{N}_R = \sum_{\boldsymbol{k},\sigma} \hat{c}^\dagger_{\boldsymbol{k}R,\sigma} \hat{c}_{\boldsymbol{k}R,\sigma}. \tag{B2}$$

The Josephson current can be defined as

$$I_J = \frac{2e}{\hbar} \mathrm{Im}\left\{ \exp\frac{-2ietV_e}{\hbar} \Phi_{\mathrm{ret}}(eV_e) \right\}, \tag{B3}$$

with

$$\Phi(i\omega) = -\int_0^{\beta\hbar} d\tau \frac{\exp i\omega_n \tau}{\hbar} \langle T_\tau \hat{A}(\tau)\hat{A}(0)\rangle, \tag{B4}$$

$$\hat{A}(t) = \sum_{\boldsymbol{k},\boldsymbol{p},\sigma} T_{\boldsymbol{k}\boldsymbol{p}} \hat{c}^\dagger_{\boldsymbol{k}\sigma}(t)\hat{c}_{\boldsymbol{p}\sigma}(t), \tag{B5}$$

where $\boldsymbol{k}$ represents the particles' momentum in the right and $\boldsymbol{p}$ in the left. $\Phi_{\mathrm{ret}}(i\omega)$ is the retarded correlation function of $\Phi(i\omega)$ and can be calculated by the analytic continuation. The tunneling of the Josephson junction is composed of two parts (one is from pair tunneling and the other is single electron tunneling)[16] and the current, I_J, is from the former. The Green's function $\mathscr{F}$, $\mathscr{F}^\dagger$ is produced by the factoring

$$\Phi(i\omega) = 2\sum_{\boldsymbol{k},\boldsymbol{p}} T_{\boldsymbol{k}\boldsymbol{p}} T_{-\boldsymbol{k},-\boldsymbol{p}} \int_0^{\beta\hbar} d\tau \frac{\exp i\omega_n \tau}{\hbar} \times \mathscr{F}^\dagger(\boldsymbol{k},\tau)\mathscr{F}(\boldsymbol{p},-\tau), \tag{B6}$$

where

$$\mathscr{F}(\boldsymbol{k},\tau)^\dagger \equiv \langle T_\tau[\hat{c}^\dagger_{\boldsymbol{k}\uparrow}(\tau)\hat{c}^\dagger_{-\boldsymbol{k}\downarrow}(0)]\rangle, \tag{B7}$$

and its conjugates

$$\mathscr{F}(\boldsymbol{p},\tau) \equiv \langle T_\tau[\hat{c}_{-\boldsymbol{p}\downarrow}(0)\hat{c}_{\boldsymbol{p}\uparrow}(\tau)]\rangle. \tag{B8}$$

With the approximation $u_{\boldsymbol{k}} \gg v_{\boldsymbol{k}}$, for the electrons above the Fermi surface,

$$\mathscr{F}(\boldsymbol{k},\tau)^\dagger \approx F(\boldsymbol{k},\tau)^\dagger \equiv u^2_{\boldsymbol{k}} \langle T_\tau[\hat{\gamma}^\dagger_{\boldsymbol{k}\uparrow}(\tau)\hat{\gamma}^\dagger_{-\boldsymbol{k}\downarrow}(0)]\rangle, \tag{B9}$$

and its conjugates

$$\mathscr{F}(\boldsymbol{p},\tau) \approx F(\boldsymbol{p},\tau) \equiv u^2_{\boldsymbol{p}} \langle T_\tau[\hat{\gamma}_{-\boldsymbol{p}\downarrow}(0)\hat{\gamma}_{\boldsymbol{p}\uparrow}(\tau)]\rangle. \tag{B10}$$

With Eqs. (B9) and (B10) and the Fourier-transformed F and $F^\dagger$, equation (B6) becomes

$$\Phi(i\omega) = 2\sum_{\boldsymbol{k},\boldsymbol{p}} T_{\boldsymbol{k}\boldsymbol{p}} T_{-\boldsymbol{k},-\boldsymbol{p}} \sum_{ip} \frac{1}{\hbar^2\beta} F^\dagger(\boldsymbol{k},ip)F(\boldsymbol{p},ip-i\omega). \tag{B11}$$

The Green's function F can be obtained by calculating its time derivative and the result is

$$F^\dagger = \frac{-\Delta' G}{ip + E_{\boldsymbol{k}}/\hbar}, \tag{B12}$$

where

$$\Delta' = \left\langle \frac{V_s \hat{b}^\dagger_0}{\hbar\sqrt{n_0}} \right\rangle. \tag{B13}$$

The Δ' can be interpreted as the superconducting gap, since when Δ' equals to zero, the Josephson current vanishes. The exact form of Δ' is not calculated since it contains the phenomenological parameter V_s. The value of Δ' is estimated as $\Delta_0/\hbar$. The simplest case at $T = 0$ K is studied at which $\Gamma = 0$ and $f(E) = 0$ for $E > E_F$, where $f(E)$ is the Fermi function, so the Matsubara sum in Eq. (B11) is

$$\sum_{ip} \frac{1}{\hbar^2\beta} F^\dagger(\boldsymbol{k},ip)F(\boldsymbol{p},ip-i\omega) = \frac{\Delta_s^2}{4E_{\boldsymbol{k}}E_{\boldsymbol{p}}\hbar} u^2_{\boldsymbol{k}} u^2_{\boldsymbol{p}} \left(\frac{1}{i\omega + \frac{E_{\boldsymbol{p}}}{\hbar} + \frac{E_{\boldsymbol{k}}}{\hbar}} - \frac{1}{i\omega - \frac{E_{\boldsymbol{p}}}{\hbar} - \frac{E_{\boldsymbol{k}}}{\hbar}} \right). \tag{B14}$$

Combined with Eqs. (B14) and (B11), equations (B3) yields

$$I_J = I_c \sin\phi, \tag{B15}$$

with

$$I_c = \frac{K\Delta_s}{2\pi e} G_n, \tag{B16}$$

$$G_n = \frac{4\pi e^2}{\hbar} |T|^2 D_L(E_F) D_R(E_F), \tag{B17}$$

where $K = 2\log 2 + 4c + \pi^2/4$, c is the Catalan constant, and T is the tunneling parameter determined by the apparatus and $|T| \approx 10^{-7}$ eV. $D_{L,R}(E_F)$ is the density of states of the left or right lead near Fermi level in normal states. The Kulik's formula for the critical Josephson current is

$$I_c = \max_{0<\phi<2\pi} \frac{\pi\Delta_s}{e} G_n \sin\frac{\phi}{2} \tanh\frac{\Delta_s \cos\frac{\phi}{2}}{2k_B T}. \tag{B18}$$

Appendix C

The calculations partly overlap with those in Ref. [15]. We focus on the denominator of the spectral weight function, $(w - \sqrt{\Delta_0^2 + (\frac{k^2}{2m})^2} - \Sigma')^2 + \Gamma^2$, where we set $\hbar = 1$. If the denominator equals to zero, we have four solutions of the momentum k in the upper half-plane of the complex plane and two solutions in the right half. For the two solutions, there are four different cases

$$a > 0, \quad b > 0; \tag{C1}$$

$$a > 0, \quad b < 0; \tag{C2}$$

$$a < 0, \quad b > 0; \tag{C3}$$

$$a < 0, \quad b < 0, \tag{C4}$$

where $a=(\omega-\Sigma')^2-\Gamma^2-\Delta_0^2$ and $b=2\Gamma(\omega-\Sigma')$.

For the first case, the two solutions of the momentum k in the right upper half-plane are

$$k_1=\sqrt{2m}R^{1/4}\exp\frac{\theta \mathrm{i}}{4}, \tag{C5}$$

$$k_2=\mathrm{i}\sqrt{2m}R^{1/4}\exp\frac{-\theta \mathrm{i}}{4}, \tag{C6}$$

where $\theta=\arctan(b/a)$ and $R=\sqrt{a^2+b^2}$. For the second case,

$$k_1=\sqrt{2m}R^{1/4}\exp\frac{-\theta \mathrm{i}}{4}, \tag{C7}$$

$$k_2=\mathrm{i}\sqrt{2m}R^{1/4}\exp\frac{\theta \mathrm{i}}{4}. \tag{C8}$$

For the third case,

$$k_1=\sqrt{2m}R^{1/4}\exp\frac{(\theta+\pi)\mathrm{i}}{4}, \tag{C9}$$

$$k_2=\mathrm{i}\sqrt{2m}R^{1/4}\exp\frac{(-\theta-\pi)\mathrm{i}}{4}. \tag{C10}$$

For the fourth case,

$$k_1=\sqrt{2m}R^{1/4}\exp\frac{(-\theta+\pi)\mathrm{i}}{4}, \tag{C11}$$

$$k_2=\mathrm{i}\sqrt{2m}R^{1/4}\exp\frac{(\theta-\pi)\mathrm{i}}{4}. \tag{C12}$$

After applying Jordan's lemma and the residue theorem, we obtain the density of states, for case one,

$$D(\omega)=\frac{mS}{2\pi}\left[\frac{\omega-\Sigma'}{\sqrt{R}}\cos\left(\frac{\theta}{2}\right)+\frac{\Gamma}{\sqrt{R}}\sin\left(\frac{\theta}{2}\right)\right]. \tag{C13}$$

For case two,

$$D(\omega)=-\frac{mS}{2\pi}\left[\frac{\omega-\Sigma'}{\sqrt{R}}\cos\left(\frac{\theta}{2}\right)+\frac{\Gamma}{\sqrt{R}}\sin\left(\frac{\theta}{2}\right)\right]. \tag{C14}$$

For case three,

$$D(\omega)=\frac{mS}{2\pi}\left[\frac{\omega-\Sigma'}{\sqrt{R}}\cos\left(\frac{\theta+\pi}{2}\right)+\frac{\Gamma}{\sqrt{R}}\sin\left(\frac{\theta+\pi}{2}\right)\right]. \tag{C15}$$

For case four,

$$D(\omega)=-\frac{mS}{2\pi}\left[\frac{\omega-\Sigma'}{\sqrt{R}}\cos\left(\frac{\theta-\pi}{2}\right)+\frac{\Gamma}{\sqrt{R}}\sin\left(\frac{\theta-\pi}{2}\right)\right]. \tag{C16}$$

References

[1] Schooley J F, Hosler W R, Ambler E, Becker J H, Cohen M L and Koonce C S 1965 *Phys. Rev. Lett.* **14** 305

[2] Noland J A 1954 *Phys. Rev.* **94** 3 724

[3] Richter C, Boschker H, Dietsche W, Fillis-Tsirakis E, Jany R, Loder F, Kourkoutis L F, Muller D A, Kirtley J R, Schneider C W and Mannhart J 2013 *Nature* **502** 528

[4] Lin X, Zhu Z, Fauque B and Behnia K 2013 *Phys. Rev. X* **3** 021002

[5] Burns G 1980 *Solid State Communications* **35** 811

[6] Arce-Gamboa J R and Guzmán-Verri G G 2018 *Phys. Rev. Mater.* **2** 104804

[7] Edge J M, Kedem Y, Aschauer U, Spaldin N A and Balatsky A V 2015 *Phys. Rev. Lett.* **115** 247002

[8] Kedem Y 2018 *Phys. Rev. B* **98** 220505

[9] Ruhman J and Lee P A 2016 *Phys. Rev. B* **94** 224515

[10] Liu B and Hu X 2010 *Phys. Rev. B* **81** 144504

[11] Monteiro A M R V L, Groenendijk D J, Manca N, Mulazimoglu E, Goswami S, Blanter Y, Vandersypen L M K and Caviglia A D 2017 *Nano Letters* **17** 715

[12] Cheng G, Tomczyk M, Lu S, Veazey J P, Huang M, Irvin P, Ryu S, Lee H, Eom C B, Hellberg C S and Levy J 2015 *Nature* **521** 196

[13] Singh G, Jouan A, Benfatto L, Couëdo F, Kumar P, Dogra A, Budhani R C, Caprara S, Grilli M, Lesne E, Barthelemy A, Bibes M, Feuillet-Palma C, Lesueur J and Bergeal N 2018 *Nat. Commun.* **9** 407

[14] Taylor P L and Heinonen O 2002 *A Auantum Approach to Condensed Matter Physics* (1st Edn.) (Cambridge: Canbridge University Press)

[15] Yang X, Liu Q H, Janko B, *et al.* unpublished

[16] Mahan G D 2000 *Many-Particle Physics* (3rd Edn.) (New York: Springer)